Supplementary information

Tubulin mRNA stability is sensitive to change in microtubule dynamics caused by multiple physiological and toxic cues

Ivana Gasic*[1], Sarah A. Boswell[2], and Timothy J. Mitchison[1]

1. Department of Systems Biology, Harvard Medical School, Boston, Massachusetts, USA

2. Department of Systems Biology, Program in Therapeutic Sciences, Harvard Medical School, Boston, Massachusetts, USA

* Correspondence to Ivana_Gasic@hms.harvard.edu

Supplementary figure legends

Supplementary Figure 1. Sub-threshold and saturating effect of microtubule drugs on microtubules in quiescent RPE 1 hTert cells. a) Cell cycle profiles of cycling and quiescent RPE 1 hTert cells treated with DMSO, or microtubule drugs (x-axis). **b and c)** Biochemical partitioning of tubulin into soluble (S) and polymerized (P) in quiescent RPE 1 hTert cells treated with DMSO control, and microtubule drugs at indicated concentrations for 6 (b) and 24h (c). Each soluble tubulin fraction is normalized to the housekeeping gene Glyceraldehyde 3-phosphate dehydrogenase (GAPDH), and each polymerized fraction to the housekeeping gene histone H3 (HISH3). All data are normalized to DMSO-treated control cells. Plotted are average values from 3 biological replicates. **d)** Average number of EB1-positive microtubule plus-tips per cell area in cells treated with microtubule drugs at indicated concentrations (x-axis), and normalized to DMSO-treated control cells (>100 cells per condition). **e)** Representative immunofluorescence images of control and cells treated with indicated microtubule-drugs, for 24 h and stained with anti-EB1 antibody (cyan), anti-β-actin, and Hoechst (red). Bar plots in all panels represent average values, and error bars standard deviations from three independent biological replicates. * p-value<0.05, ** p-value<0.01, *** p-value<0.001 in paired Student T-test compared to DMSO control.

Supplementary Figure 2. Microtubule damage triggers differential tubulin gene expression across many cancer cell types and *in vivo*. a) Expression profiles of all detected α- and β-tubulin isoform across a panel of breast, ovarian and endometrial

cancer cell lines treated with microtubule poisons for 24h. This dataset is available on GEO database (GEO series GSE50811, GSE50830, and GSE50831[15]). Dendrogram on the left represents Pearson distance between expression profiles. Each column of the heatmap represents differential gene expression in one cell line treated with indicated microtubule drug, marked above the heatmap. Each row represents a gene, labeled on y-axis. Color key is depicted in upper left corner. Data are represented as Log_2FC relative to DMSO control. **b)** Expression profiles of all detected α- and β-tubulin isoforms in heart endothelial cells isolated from control and rats treated with microtubule poisons vinblastine (VIN), vincristine (VCR), or colchicine (COL) at indicated doses (x-axis) for 6 and 24h. This dataset is available on GEO database (GEO series GSE19290). Dendrogram on the left represents Pearson distance between expression profiles. Each column of the heatmap represents differential gene expression in one condition, labeled on the x-axis. Each row represents a gene, labeled on y-axis. Color key is depicted in upper left corner. Data are represented as Log_2FC relative to DMSO control. **c)** Experimental strategy and primer design for RT-qPCR.

Supplementary Figure 3. Nutrient deprivation regulates the expression of α- and β-tubulin isoforms transcriptionally and post-transcriptionally. a and e) DGE in control and cells deprived of D-glucose (a, A549 cell line, GEO series GSE56843[26]), or L-glutamine (e, U2OS cell line, GEO series GSE59931). Each column represents DGE in one replicate of control or nutrient deprived cells (x-axis). Each row represents one gene (y-axes). CEM 1 consists of tubulin genes with high Pearson expression correlation. Null module consists of tubulin genes with low Pearson expression correlation. Scales of

expression profile Z-scores are depicted above each heatmap. **b and f)** Relative expression of TUBA1A and TUBB unspliced pre-mRNA in control and A549 cells deprived of D-glucose (b), or control and U2OS cells deprived of L-Glutamine for indicated periods of time (f, x-axes). **c and g)** Relative expression of TUBA1A and TUBB mRNA in control and A549 cells deprived of D-glucose (c), or control and U2OS cells deprived of L-Glutamine for indicated periods of time (g, x-axis). All the relative gene expression data are normalized to housekeeping gene GAPDH or RPL19, and to time point 0h (control). **d and h)** Tubulin partitioning to unpolymerized (soluble) and polymerized (pellet), and total tubulin, normalized to loading controls: GAPDH for soluble and total, and HISH3 for pellet, in control and nutrient deprived cells for 24 hours. All data are normalized to DMSO control. Bar plots in all panels represent average values, and error bars standard deviations from three independent biological replicates. * $p<0.05$, ** $p<0.01$, *** $p<0.001$ in Paired Student T-test compared to control treatment.

Supplementary Figure 4. PI3K inhibitor BKM-120, but not BEZ-235 and GDC-1941, displays off-target effect on microtubules. a) Quantification of the number of EB-positive microtubule plus-tips per cell area in RPE 1 hTert cells treated with DMSO or indicated concentrations (x-axis) of PI3K inhibitors. Data are normalized to DMSO-treated control cells. Lines represent average number of EB signals per cell area, and shaded area represents standard error of the mean over three independent experiments and >100 cells per condition. **b)** Representative immunofluorescence images of control and cells treated with indicated 1 μM PI3K inhibitors for 6h, and stained with anti-EB1 antibody (cyan), anti-β-actin, and Hoechst (red).

Supplementary Table 1. RT-qPCR primer sequences. Listed are target mRNA species, sequences, and orientation of all the primers used for RT-qPCR in this study.

Supplementary Table 2. Perturbations that trigger tubulin differential expression. Listed are Rank based on descending Pearson expression-correlation coefficients, GEO identifiers, titles of studies, and observed Pearson expression-correlation coefficients for a subset of tubulin genes across the 417 datasets from human platform in the CLIC-report.

Supplementary Figure 1

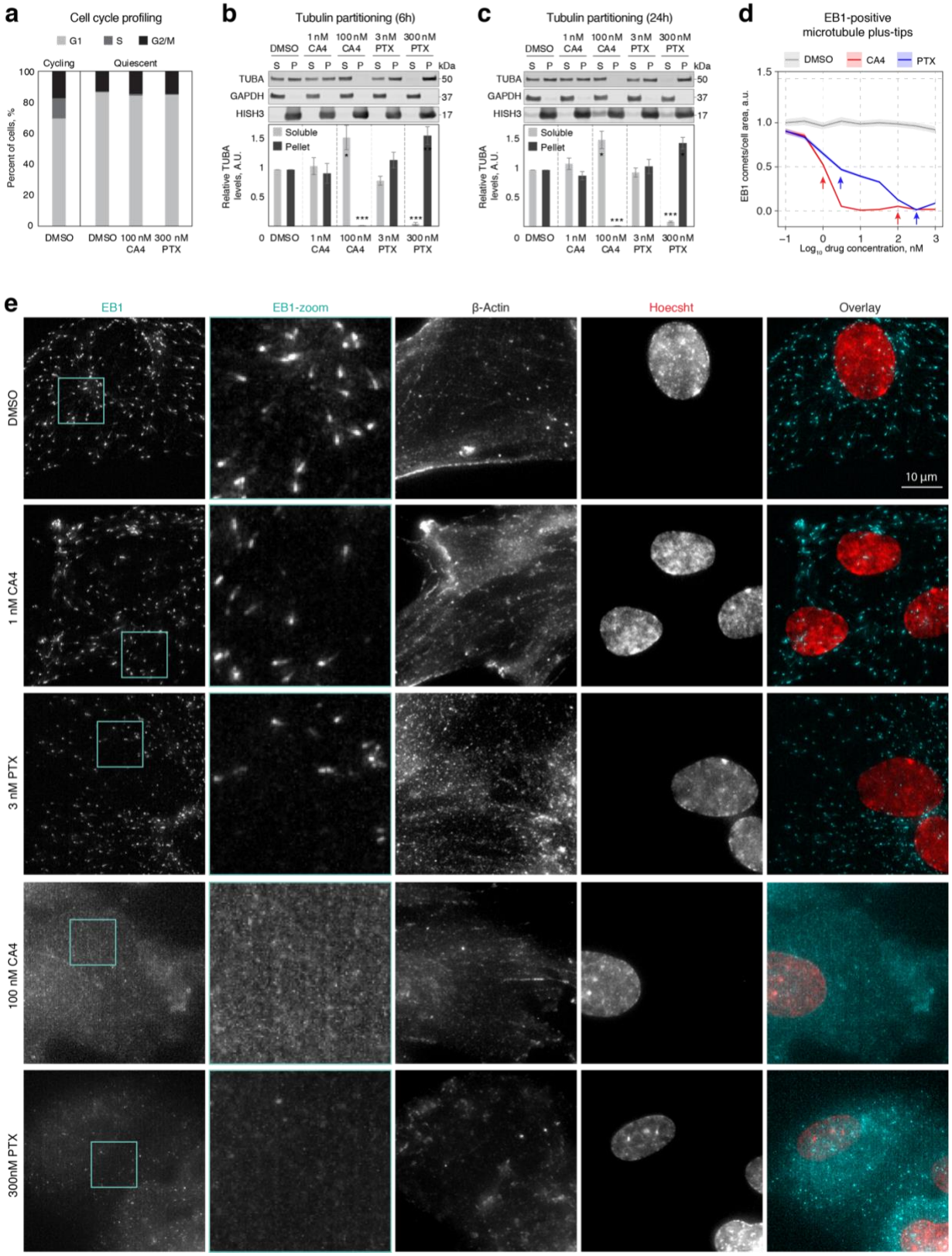

Supplementary Figure 2

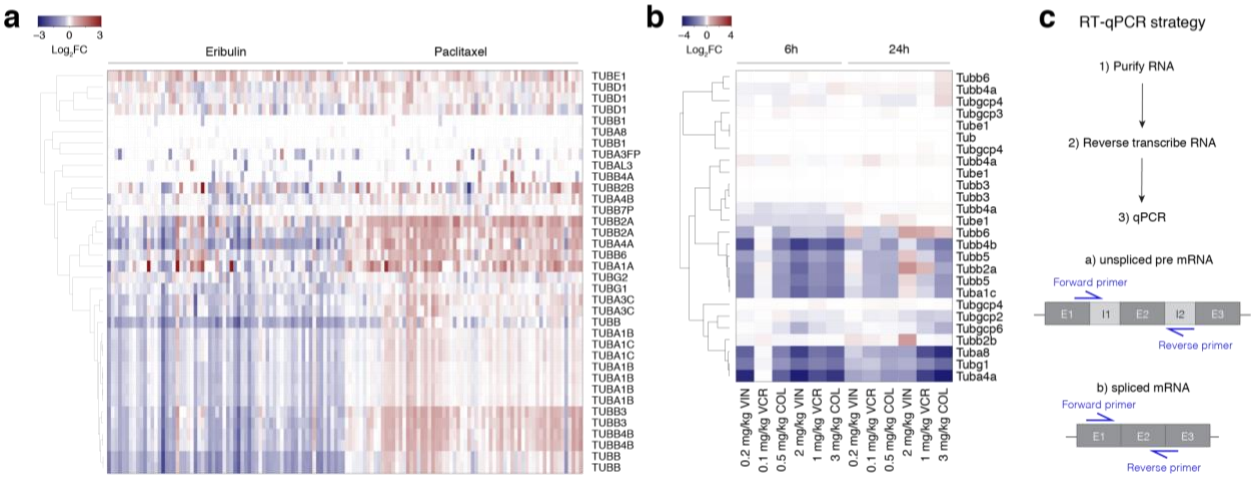

Supplementary Figure 3

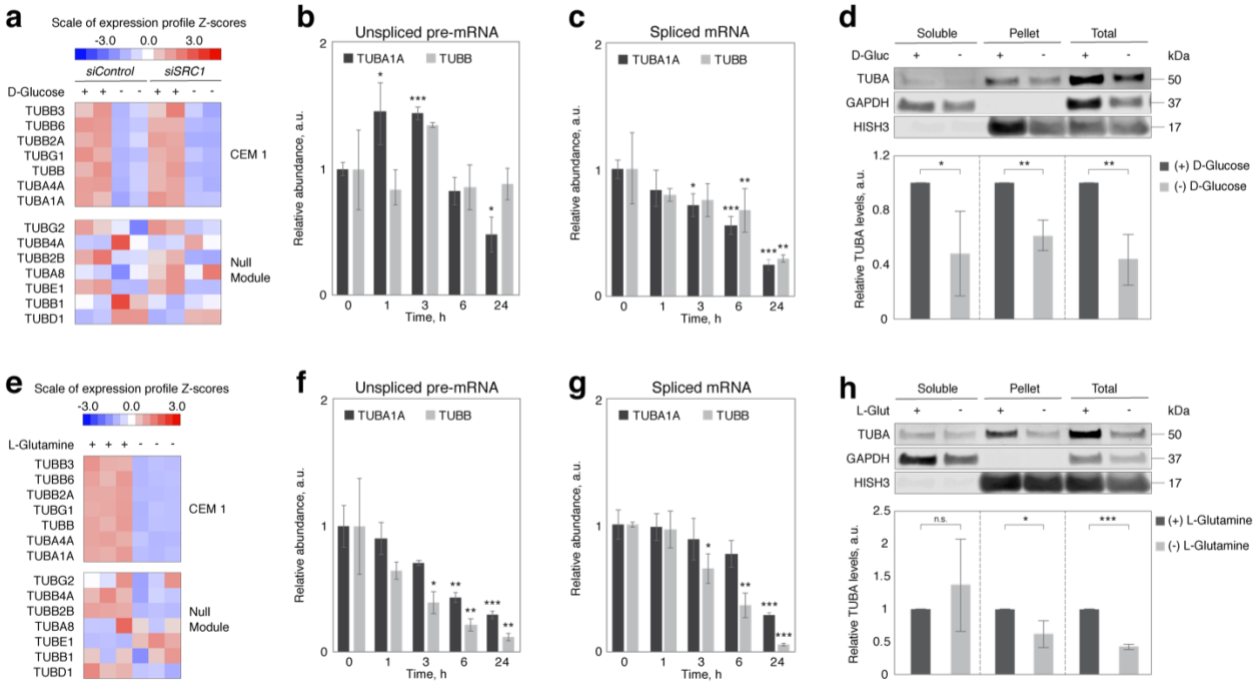

Supplementary Figure 4

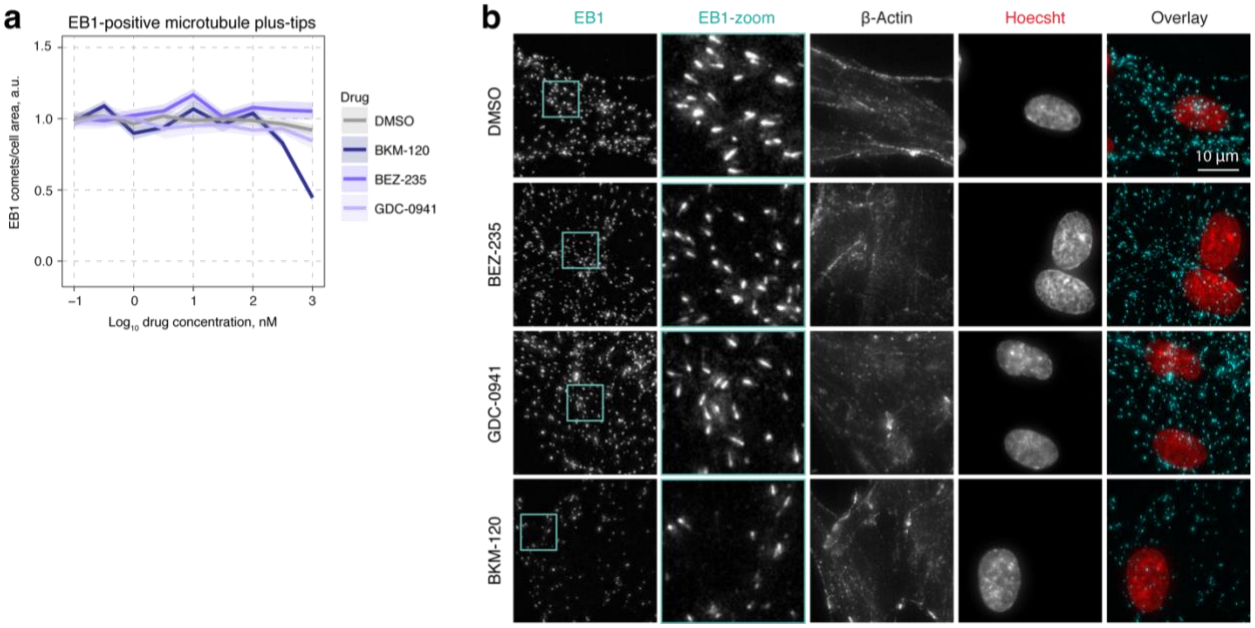

Supplementary Table 1

Gene	RNA species	Orientation	Sequence, 5'-3'
TUBA1A	pre-mRNA	forward	GCAGCATTTGTAGCAGGTGA
		reverse	GCATTGCCAATCTGGACAC
	mRNA	forward	CCACAGTCATTGATGAAGTTCG
		reverse	GCTGTGGAAAACCAAGAAGC
TUBB	pre-mRNA	forward	CTGGACCGCATCTCTGTGTA
		reverse	GGTTCACGAAAGGGACAAAA
	mRNA	forward	GAAGCCACAGGTGGCAAATA
		reverse	CGTACCACATCCAGGACAGA
GAPDH	pre-mRNA	forward	GGGAGGTAGAGGGGTGATGT
		reverse	GAGGCAGGGATGATGTTCTG
	mRNA	forward	AGCTCATTTCCTGGTATGACA
		reverse	AGGGGAGATTCAGTGTGGTG
RPL19	pre-mRNA	forward	TCCGAGAGGTGAAGGCATAG
		reverse	GCCTCTTCTGAAGCCTGAGC
	mRNA	forward	ATCGCCACATGTATCACAGC
		reverse	TTGGTCTCTTCCTCCTTGGAT

Supplementary Table 2

			Pearson Correlation Coefficient								
Rank	**GSE**	**Title of the study**	**TUBB3**	**TUBB6**	**TUBB2A**	**TUBG1**	**TUBB**	**TUBA4A**	**TUBA1A**	**TUBB4B**	**TUBA1C**
1	GSE59931	Glutamine deprivation in U2OS cells	0.98	0.99	0.99	0.99	0.99	0.98	0.99	0.99	0.91
2	GSE36529	Expression data from CtBP knockdown MCF-7 cells	0.98	0.96	0.98	0.98	0.99	0.98	0.98	0.98	0.97
3	GSE32158	Bisphenol A Regulates the Expression of DNA Repair Genes in Human Breast Epithelial Cells (expression data)	0.98	0.98	0.98	0.96	0.97	0.98	0.95	0.97	0.97
4	GSE23952	Expression data from TGF-beta treated Panc-1 pancreatic adenocarcinoma cell line	0.98	0.98	0.97	0.97	0.92	0.98	0.98	0.98	0.98
5	GSE22522	Comparison of the transcriptome of K-LEC spheroids to control LEC spheroids	0.98	0.96	0.96	0.98	0.97	0.92	0.97	0.98	0.96
6	GSE56843	Steroid Receptor Coactivator 1 is an Integrator of Glucose and NAD(+)/NADH Homeostasis	0.93	0.97	0.97	0.96	0.97	0.98	0.95	0.97	0.96
7	GSE20719	Gene expression changes upon treatment of T47D breast cancer cells with the Pan-PI3 kinase inhibitor GDC-0941	0.95	0.96	0.97	0.98	0.94	0.96	0.93	0.98	0.93
8	GSE4217	Spheroid Formation and Recovery of Human Foreskin Fibroblasts at Ambient Temperature	0.97	0.96	0.96	0.92	0.90	0.94	0.94	0.97	0.96
9	GSE58605	Expression data from A549 cells infected by adenovirus not carrying virus associated sequences in the genome.	0.94	0.92	0.94	0.94	0.93	0.95	0.96	0.96	0.57
10	GSE46708	CD24 targets	0.96	0.96	0.95	0.90	0.91	0.93	0.92	0.96	0.95
11	GSE35428	Transcriptional profiling of clinically relevant SERMs and SERM/estradiol complexes in a cellular model of breast cancer	0.95	0.95	0.92	0.95	0.92	0.93	0.91	0.96	0.95
12	GSE7745	Mapping of HNF4Œ± binding sites, acetylation of histone H3 and expression in Caco2 cells	0.94	0.94	0.94	0.87	0.94	0.88	0.88	0.94	0.95
13	GSE46924	27-Hydroxycholesterol links cholesterol and breast cancer pathophysiology.	0.90	0.93	0.92	0.95	0.93	0.90	0.84	0.93	0.88
14	GSE16659	Expression data of HGF/cMET pathway in prostate cancer DU145 cell line	0.94	0.94	0.80	0.92	0.92	0.92	0.88	0.84	0.31
15	GSE52659	Expression data from WEEV infected BE(2)-C/m cells	0.92	0.88	0.94	0.91	0.94	0.87	0.79	0.83	0.87
16	GSE10444	gene expression levels in long-term cultures of human dental pulp stem cells	0.83	0.88	0.90	0.92	0.93	0.89	0.86	0.94	0.81
17	GSE4218	Spheroid Formation and Recovery of Human T98G Glioma Cells at Ambient Temperature	0.92	0.93	0.87	0.84	0.81	0.93	0.88	0.94	0.91
18	GSE15499	HDAC5 is a repressor of angiogenesis and determines the angiogenic gene expression pattern of endothelial cells	0.90	0.84	0.86	0.93	0.94	0.82	0.91	0.92	0.86
19	GSE33143	Targeted disruption of the BCL9/beta-catenin complex in cancer	0.91	0.87	0.89	0.89	0.87	0.90	0.81	0.83	0.16
20	GSE42733	Gene expression profile of Nurse-Like Cells (NLC) derived from chronic lymphocytic leukemia	0.81	0.90	0.89	0.90	0.88	0.88	0.84	0.68	0.91
21	GSE36085	Regulation of Autophagy by VEGF-C axis in cancer	0.91	0.87	0.90	0.90	0.86	0.92	0.72	0.91	0.78
22	GSE43700	Microarray analysis of IL-10 stimulated adherent peripheral blood mononuclear cells	0.90	0.88	0.87	0.74	0.81	0.92	0.92	0.93	0.91
23	GSE29625	Human embryonic stem cells derived from embryos at different stages of development share similar transcription profiles	0.90	0.86	0.91	0.83	0.88	0.89	0.78	0.93	0.83
24	GSE12098	Comparison of the migration profile of MSCs	0.88	0.70	0.88	0.89	0.90	0.89	0.81	0.93	0.89
25	GSE13378	Exposure of squamous esophageal cell line HET-1A to deoxycholic acid (DCA)	0.85	0.74	0.90	0.87	0.85	0.87	0.87	0.89	-0.19
26	GSE32161	Microarray analysis of genes associated with cell surface NIS protein levels in breast cancer	0.88	0.81	0.91	0.90	0.79	0.79	0.87	0.88	0.87
27	GSE16070	Networking of differentially expressed genes in human MCF7 breast cancer cells resistant to methotrexate	0.90	0.90	0.79	0.77	0.83	0.84	0.90	0.92	0.73
28	GSE36176	Gene expression arrays on lung cancer cells exposed to Notch inhibitor	0.88	0.85	0.90	0.90	0.71	0.90	0.71	0.92	0.87
29	GSE23399	Gene expression profling of human breast carcinoma-associated fibroblasts treated with paclitaxol or doxorubicin at therapeutically relevant doses	0.85	0.85	0.85	0.81	0.86	0.77	0.86	0.90	0.82

30	GSE14001	PAX2: A Potential Biomarker for Low Malignant Potential Ovarian Tumors and Low-Grade Serous Ovarian Carcinomas	0.89	0.87	0.88	0.82	0.80	0.69	0.87	0.84	0.83
31	GSE17368	Epiphyseal cartilage	0.89	0.87	0.75	0.82	0.78	0.87	0.82	0.86	0.89
32	GSE19495	Global Gene Expression of Human Hepatoma Cells After Amino Acid Limitation	0.60	0.83	0.87	0.88	0.81	0.89	0.86	0.74	0.82
33	GSE14773	Roles of EMT regulator in colon cancer	0.88	0.89	0.74	0.77	0.79	0.81	0.81	0.85	0.90
34	GSE19136	Gene expression response to implanted drug (paclitaxel)-eluting or bare metal stents in denuded human LIMA arteries	0.85	0.84	0.86	0.77	0.74	0.79	0.84	0.90	0.87
35	GSE16356	Lymphatic endothelial cells (LEC) treated with a MAF-targeted siRNA	0.84	0.78	0.81	0.75	0.85	0.77	0.87	0.84	0.48
36	GSE9835	Gene Expression Changes in Response to Baculoviral Vector Transduction of Neuronal Cells In Vitro	0.62	0.87	0.82	0.79	0.89	0.87	0.76	0.87	0.68
37	GSE17044	Expression data from androgen treated LNCaP cells	0.89	0.80	0.88	0.69	0.85	0.73	0.77	0.89	0.62
38	GSE9649	Expression studies of HMEC exposed to lactic acidosis and hypoxia	0.86	0.74	0.85	0.78	0.81	0.86	0.72	0.87	0.80
39	GSE31641	Expression data from treatment of human melanocytes with phenolic compounds	0.85	0.79	0.83	0.70	0.84	0.75	0.83	0.86	0.90
40	GSE13142	HepG2/C3A cells cultured for 42 h in complete or leucine-devoid medium	0.89	0.48	0.84	0.88	0.87	0.85	0.75	0.89	0.88
41	GSE7345	Germline NRAS mutation causes a novel human autoimmune lymphoproliferative syndrome	0.86	0.66	0.73	0.83	0.86	0.83	0.75	0.88	0.87
42	GSE34635	Defining a No Observable Transcriptional Effect Level (NOTEL) for low dose N-OH-PhIP exposures in human BEAS-2B bronchioepithelial cells	0.84	0.82	0.82	0.79	0.50	0.86	0.86	0.86	0.81
43	GSE5838	Expression data from transplanted intestine bifor signs of rejection, and when their was signs of rejection	0.86	0.58	0.72	0.86	0.80	0.87	0.79	0.88	0.89
44	GSE51130	Using a rhabdomyosarcoma patient-derived xenograft to examine precision medicine approaches and model acquired resistance	0.88	0.57	0.85	0.76	0.80	0.84	0.79	0.89	0.76
45	GSE34512	PBEF Knockdown in HMVEC-LBI	0.87	0.88	0.84	0.84	0.84	0.80	0.39	0.89	0.46
46	GSE42853	Distinct gene expression profiles associated with the susceptibility of pathogen-specific CD4 T cells to HIV-1 infection	0.86	0.65	0.83	0.81	0.86	0.58	0.87	0.89	0.89
47	GSE26884	Bisphenol A Induced the Expression of DNA Repair Genes in Human Breast Epithelial Cells	0.80	0.84	0.80	0.62	0.83	0.88	0.67	0.76	0.76
48	GSE53731	Expression data from hepatitis E virus inoculated PLC/PRF/5 cells	0.77	0.85	0.75	0.85	0.73	0.65	0.83	0.78	0.82
49	GSE8588	OH-PBDE-induced gene expression profiling in H295R adrenocortical carcinoma cells	0.87	0.52	0.85	0.69	0.83	0.82	0.85	0.88	0.82
50	GSE12875	Impaired T-cell function in patients with novel ICOS	0.86	0.52	0.87	0.83	0.82	0.77	0.75	0.88	0.83
51	GSE45636	eIF3a in Urinary Bladder Cancer ‚Äì in vivo and in vitro insights	0.87	0.84	0.81	0.54	0.86	0.81	0.68	0.83	0.72
52	GSE49085	Identification of bone morphogenetic protein (BMP)-7 as a key instructive factor for human epidermal Langerhans cell differentiation and proliferation	0.84	0.82	0.84	0.86	0.76	0.60	0.68	0.85	0.81
53	GSE31472	Host cell gene expression in Influenza A/duck/Malaysia/F118/08/2004 (H5N2) infected A549 cells at 2, 4, 6, 8, and 10 hours post infection	0.80	0.84	0.84	0.56	0.86	0.80	0.69	0.88	-0.37
54	GSE9677	Gene expression profile in HUVECs before and after Angiopoietin stimulation	0.83	0.86	0.85	0.85	0.73	0.83	0.44	0.87	0.69
55	GSE6400	Cultured A549 lung cancer cells treated with actinomycin D and sapphyrin PCI-2050	0.83	0.81	0.85	0.78	0.58	0.79	0.71	0.77	0.53
56	GSE16089	Networking of differentially expressed genes in human Saos-2 osteosarcoma cells resistant to methotrexate	0.85	0.73	0.36	0.85	0.86	0.86	0.85	0.89	0.89
57	GSE15065	C/EBPbeta-2 regulation of gene expression in MCF10A cells	0.86	0.82	0.78	0.74	0.80	0.83	0.49	0.86	0.82
58	GSE5110	48h Immobilization in human	0.77	0.73	0.73	0.84	0.61	0.81	0.82	0.87	0.76
59	GSE44540	Gene expression in hTERT-RPE1 cells with overexpression of MFRP	0.85	0.84	0.79	0.86	0.39	0.75	0.84	0.89	0.83
60	GSE23764	Expression data from actomyosin contractility regulated genes	0.80	0.69	0.82	0.77	0.72	0.80	0.70	0.86	0.72
61	GSE20037	cdr2 siRNA knockdown during passage through mitosis: HeLa cells, Rat1 wild type and c-myc null cells	0.80	0.46	0.82	0.79	0.79	0.82	0.80	0.70	0.47

62	GSE40517	Selective Requirement for Mediator MED23 in Ras-active Lung Cancer	0.79	0.75	0.84	0.65	0.82	0.77	0.65	0.71	0.79
63	GSE19510	Transcriptional response of normal human lung WI-38 fibroblasts to benzo[a]pyrene diol epoxide: a dose-response study	0.82	0.86	0.66	0.64	0.79	0.73	0.77	0.85	0.88
64	GSE17785	Endogenous expression of an oncogenic PI3K mutation leads to activated PI3K pathway signaling and an invasive phenotype	0.83	0.82	0.81	0.51	0.78	0.81	0.65	0.86	0.80
65	GSE29384	Tetracycline-Inducible Cyr61 effect on LN229 glioma cells	0.79	0.83	0.84	0.83	0.83	0.25	0.83	0.86	0.68
66	GSE28339	Gene expression data following Cyclin T2 and Cyclin T1 depletion by shRNA in HeLa cells	0.83	0.81	0.53	0.54	0.83	0.83	0.76	0.83	0.65
67	GSE2328	Application of genome-wide expression analysis to human health & disease	0.77	0.78	0.76	0.36	0.83	0.80	0.81	0.85	0.78
68	GSE33606	Gene expression changes in human hepatocytes exposed to VX (O-ethyl S-[2-(diisopropylamino)ethyl] methylphosphonothiolate)	0.82	0.77	0.81	0.53	0.84	0.75	0.54	0.86	0.84
69	GSE37648	Gene signatures of normal hTERT immortalized ovarian epithelium and fallopian tube epithelium (paired cultures from 2 donor patients)	0.84	0.77	0.71	0.74	0.75	0.77	0.50	0.79	0.82
70	GSE45417	Expression data from knockdown of ZXDC1/2 in PMA-treated U937	0.79	0.74	0.75	0.79	0.74	0.81	0.45	0.80	0.85
71	GSE37474	Dexamethasone induced gene expression changes in the human trabecular meshwork	0.79	0.78	0.74	0.72	0.74	0.57	0.69	0.83	0.77
72	GSE24224	Analysis of genome-wide methylation and gene expression induced by decitabine treatment in HL60 leukemia cell line	0.70	0.80	0.81	0.62	0.51	0.78	0.82	0.63	0.51
73	GSE26599	Gene expression profile in response to doxorubicin-rapamycin combined treatment of HER-2 overexpressing human mammary epithelial cell lines	0.82	0.81	0.81	0.78	0.79	0.55	0.47	0.81	0.62
74	GSE20125	Transcriptome analysis of human Wharton,Äôs jelly stem cells: meta-analysis	0.75	0.73	0.70	0.80	0.77	0.48	0.72	0.84	0.81
75	GSE47874	The Heritage (HEalth, RIsk factors, exercise Training And GEnetics) family study	0.75	0.64	0.77	0.74	0.77	0.63	0.66	0.78	0.79
76	GSE6494	Expression data from human liver cell line induced by PCB153	0.80	0.75	0.63	0.57	0.75	0.65	0.78	0.75	0.59
77	GSE38517	Expression data from fibroblasts derived from human normal oral mucosa, oral dysplasia and oral squamous cell carcinoma	0.82	0.82	0.73	0.75	0.73	0.64	0.41	0.82	0.81
78	GSE33243	Human acute myelogenous leukemia-initiating cells treated with fenretinide	0.78	0.46	0.66	0.73	0.68	0.76	0.81	0.80	0.73
79	GSE22533	Breast cancer cells resistant to hormone deprivation maintain an estrogen receptor alpha-dependent, E2F-directed transcriptional program	0.81	0.83	0.78	0.82	0.81	0.41	0.40	0.85	0.85
80	GSE30494	Expression data in cancer cell lines using Affymetrix GeneChip	0.63	0.79	0.80	0.79	0.36	0.69	0.76	0.79	-0.37
81	GSE4824	Analysis of lung cancer cell lines	0.77	0.80	0.69	0.45	0.80	0.60	0.70	0.78	0.81
82	GSE15372	Expression data from A2780 (cisplatin-sensitive) and Round5 A2780 (cisplatin-resistant) cell lines.	0.53	0.78	0.82	0.76	0.79	0.48	0.64	0.81	0.47
83	GSE16524	Expression data from skin fibroblasts derived from Setleis Syndrome patients and normal controls	0.81	0.68	0.70	0.73	0.72	0.66	0.50	0.84	0.72
84	GSE13054	Genes upregulated by HLX	0.82	0.37	0.70	0.69	0.78	0.75	0.68	0.80	0.80
85	GSE12274	Mesenchymal Stromal Cells of Different Donor Age	0.80	0.82	0.53	0.71	0.77	0.60	0.56	0.84	0.79
86	GSE35170	Expression data from U87-2M1 glioma cells transduced with baculoviral control decoy vector or baculoviral miR-10b decoy vector	0.78	0.71	0.68	0.38	0.72	0.73	0.77	0.80	0.41
87	GSE20540	Gene expression profiles of myeloma cells interacting with bone marrow stromal cells in vitro	0.72	0.68	0.73	0.75	0.76	0.34	0.76	0.36	0.37
88	GSE4289	Host transcriptome changes associated with episome loss and selection of keratinocytes containing integrated HPV16	0.77	0.80	0.80	0.62	0.57	0.78	0.39	0.71	0.79
89	GSE11352	Timecourse of estradiol (10nM) exposure in MCF7 breast cancer cells.	0.73	0.66	0.77	0.69	0.61	0.58	0.67	0.77	0.56
90	GSE39999	Filarial nematode AsnRS interacts with interleukin 8 receptors in iDCs but causes different gene expression patterns compared to iDCs stimulated by interleukin 8.	0.72	0.75	0.74	0.72	0.73	0.58	0.66	0.80	0.81

91	GSE11208	Chronic nicotine exposure (kuo-affy-human-232930)	0.70	0.72	0.47	0.75	0.72	0.67	0.65	0.68	0.70
92	GSE14986	Antiestrogen-resistant subclones of MCF-7 human breast cancer cells are derived from a common clonal drug-resistant progenitor	0.70	0.57	0.66	0.62	0.74	0.73	0.67	0.74	0.62
93	GSE16538	Genome-wide gene expression profile analysis in pulmonary sarcoidosis	0.75	0.67	0.71	0.70	0.73	0.68	0.42	0.70	0.71
94	GSE18182	Expression profile of lung adenocarcinoma, A549 cells following targeted depletion of non metastatic 2 (NME2/NM23 H2)	0.74	0.62	0.46	0.70	0.81	0.71	0.61	0.75	-0.05
95	GSE32892	A genome-wide and dose-dependent inhibition map of androgen receptor binding by small molecules reveals its regulatory program upon antagonism	0.74	0.78	0.76	0.81	0.76	0.68	0.11	0.82	0.78
96	GSE40220	INTESTINAL FILTER FOR USE IN OESOPHAGEAL CANCER RESEARCH	0.73	0.80	0.74	0.75	0.67	0.80	0.14	0.74	0.75
97	GSE33146	Expression data from DKAT breast cancer cell line pre- and post-EMT	0.78	0.72	0.74	0.74	0.52	0.69	0.45	0.63	-0.09
98	GSE17624	Expression data from human Ishikawa cells treated with Bisphenol A	0.73	0.78	0.60	0.61	0.75	0.72	0.43	0.80	0.39
99	GSE17090	Expression data from human adipose stem cells expanded in allogeneic human serum and fetal bovine serum	0.77	0.72	0.75	0.72	0.50	0.59	0.52	0.78	0.80
100	GSE16054	Transient expression of misfolded surfactant protein C	0.56	0.56	0.79	0.76	0.75	0.70	0.41	0.76	0.69
101	GSE16715	Expression profiling in Williams-Beuren Syndrome patient fibroblast cell lines	0.76	0.61	0.62	0.52	0.73	0.58	0.70	0.78	0.73
102	GSE9593	Cellular Aging of Mesenchymal Stem Cells	0.75	0.77	0.40	0.63	0.78	0.74	0.43	0.79	0.73
103	GSE7846	Differentially expressed genes in HEECs of eutopic endometrium of patients with endometriosis compared with control	0.72	0.69	0.77	0.62	0.64	0.35	0.67	0.80	0.70
104	GSE13671	Expression data from mammary epithelial cells from BRCA1 mutation carriers and non BRCA1 mutation carriers	0.75	0.70	0.54	0.61	0.51	0.72	0.65	0.67	0.75
105	GSE8045	Gene Expression Profiling in A549 Lung Cancer Cell Line Following siRNA Mediated Knock-down of ALDH1A1 and ALDH3A1	0.78	0.75	0.70	0.72	0.67	0.16	0.70	0.80	0.81
106	GSE11550	Hs 294T Cells Treated with Elesclomol Alone or in Combination with Paclitaxel Compared to DMSO Treated	0.70	0.48	0.76	0.49	0.74	0.65	0.66	0.81	0.54
107	GSE6869	Expression data from human liver cell line induced by PCB77	0.72	0.76	0.51	0.66	0.70	0.66	0.45	0.75	0.64
108	GSE51549	All trans-retinoic acid (ATRA) re-differentiate early transformed breast epithelial cells to normal.	0.79	0.69	0.73	0.40	0.46	0.70	0.67	0.80	0.66
109	GSE32939	CD4 on human monocytes	0.80	0.42	0.59	0.69	0.41	0.78	0.77	0.83	0.73
110	GSE16547	KSHV Manipulates Notch Signaling by Upregulating Dll4 and JAG1 to Alter Cell Cycle Gene Expression in LECs	0.75	0.70	0.74	0.71	0.73	0.75	0.06	0.77	0.75
111	GSE14807	Investigation of over-expressing Annexin receptor cell line with and without agonists	0.57	0.75	0.69	0.75	0.60	0.66	0.76	0.59	0.37
112	GSE18161	Washing scaling of microarray expression	0.63	0.74	0.66	0.42	0.71	0.53	0.69	0.72	0.71
113	GSE9361	Functional interaction between a PIP2 novel polyA polymerase and type 1 PIPKIalpha	0.71	0.73	0.62	0.73	0.08	0.75	0.75	0.78	0.71
114	GSE33455	Expression data from docetaxel-resistant prostate cancer cell lines	0.52	0.77	0.68	0.76	0.78	0.66	0.18	0.70	-0.16
115	GSE32984	Gene expression profiling of Human Umbilical Vein Endothelial Cells (HUVEC) after treatment with Erg or control antisense (GeneBloc)	0.66	0.72	0.63	0.47	0.75	0.70	0.42	0.75	0.65
116	GSE30038	Programming human pluripotent stem cells into adipocytes [Affymetrix]	0.68	0.75	0.74	0.39	0.75	0.35	0.74	0.69	0.62
117	GSE35957	Effects of Cellular Senescence on Human Mesenchymal Stem Cells	0.63	0.62	0.64	0.73	0.70	0.50	0.49	0.77	0.76
118	GSE10934	Human sclera	0.71	0.74	0.69	0.75	0.73	0.02	0.68	0.79	0.76
119	GSE18892	Silencing of AEBP1 in U87MG glial cells and Chip-chIP with AEBP1 antibody	0.78	0.71	0.70	0.58	0.45	0.65	0.57	0.78	0.75
120	GSE47873	Gene expression profiles MCF-10A cells overexpressing MBD2	0.79	0.76	0.39	0.74	0.69	0.75	0.17	0.78	0.80
121	GSE31469	Host cell gene expression in Influenza A/WSN/33 (H1N1) infected A549 cells at 2, 4 and 6 hours post infection	0.71	0.32	0.64	0.52	0.67	0.72	0.71	0.77	0.25
122	GSE28448	Antagonistic regulation of EMT by TIF1Œ≥ and Smad4 in mammary epithelial cells	0.56	0.74	0.73	0.59	0.65	0.73	0.30	0.66	0.71

123	GSE18866	Expression data from doxycylin-inducible miR-15a/16-1 and empty vector (EV) expression in a 13q14-\- cell line	0.68	0.71	0.44	0.72	0.30	0.74	0.70	0.76	0.28
124	GSE28829	Gene Expression in early and advanced atherosclerotic plaque from human carotid	0.71	0.72	0.68	0.66	0.45	0.44	0.59	0.76	0.65
125	GSE9768	Identification of genes modulated by acid and bile in a Barrett's oesophagus cell line	0.75	0.69	0.11	0.74	0.75	0.71	0.52	0.76	0.47
126	GSE7700	Genes regulated by YAP in normal breast cell line and breast cancer cell lines	0.76	0.74	0.74	0.76	0.73	-0.24	0.76	0.79	0.80
127	GSE16962	Effect of mir-210 overexpression or down-modulation on human umbilical vein cells	0.72	0.70	0.75	0.72	0.31	0.75	0.31	0.73	0.72
128	GSE21570	Frizzled 4 regulates stemness and invasiveness of migrating glioma cells established by serial in vivo intracranial transplantation	0.66	0.77	0.75	0.63	0.67	0.72	0.36	0.65	0.71
129	GSE25746	Integrated, genome-wide screening for hypomethylated oncogenes in salivary gland adenoid cystic carcinoma	0.72	0.73	0.12	0.69	0.63	0.57	0.76	0.75	0.76
130	GSE27200	Expression data from Sotos syndrome patients and controls	0.73	0.66	0.54	0.58	0.63	0.53	0.54	0.74	0.78
131	GSE61352	Expression data from normal urothelial cells with exogenous expression of mutant FGFR3	0.32	0.75	0.78	0.70	0.63	0.78	0.61	0.48	0.72
132	GSE7824	Zonal Heterogeneity for Gene Expression in Human Pancreatic Carcinoma Growing in the Pancreas of Nude Mice	0.69	0.68	0.62	0.62	0.54	0.61	0.45	0.68	0.62
133	GSE17466	Gene expression in iPrEC cell line transfected with wild-type USP2A, mutant USP2A, or empty vector.	0.73	0.62	0.39	0.68	0.67	0.69	0.43	0.76	0.67
134	GSE29265	Sporadic vs. Post-Chernobyl Papillary vs. Anaplastic Thyroid Cancers	0.65	0.66	0.64	0.57	0.64	0.44	0.59	0.48	0.74
135	GSE42762	FOXO3a Is A Major Target Of Inactivation By PI3K/AKT Signaling In Aggressive Neuroblastoma	0.71	0.68	0.67	0.75	0.72	0.57	0.09	0.79	0.53
136	GSE30336	Expression analysis of 52 glioma clinical samples (36 CIMP+ and 16 CIMP-) and 6 cell line samples	0.68	0.56	0.79	0.76	0.63	0.40	0.62	0.66	0.42
137	GSE33168	The amniotic fluid transcriptome: a source of novel information about human fetal development	0.48	0.66	0.72	0.53	0.65	0.47	0.67	0.71	0.18
138	GSE6460	Human mesenchymal stem cells	0.67	0.67	0.74	0.65	0.73	0.59	0.12	0.68	0.49
139	GSE57441	Genes expression of cervical squamous cell carcinoma, CaSki cells, treated with or without recombinant TGF-b1 (2 ng/mL)	0.66	0.73	0.70	-0.02	0.71	0.67	0.70	0.23	-0.28
140	GSE40611	Gene expression data of parotid tissue from Primary Sjogren‚Äôs Syndrome and controls	0.67	0.55	0.56	0.58	0.61	0.70	0.47	0.74	0.73
141	GSE6679	Staufen1 regulates a variety of mammalian transcripts	0.68	0.76	0.60	0.73	0.30	0.77	0.53	0.38	-0.11
142	GSE36970	KDM4B- and KDM6B-regulated genes in human mesenchymal stem cell osteogenic differentiation	0.71	0.67	0.74	0.28	0.49	0.53	0.67	0.79	0.79
143	GSE30391	Expression data from human Wharton's jelly stem cells	0.65	0.69	0.64	0.47	0.70	0.43	0.48	0.73	0.66
144	GSE7807	Leukotriene D4 induces gene expression in human monocytes through cysteinyl leukotriene type I receptor.	0.69	0.64	0.74	0.43	0.71	0.34	0.59	0.65	0.57
145	GSE35382	Comparison of gene expression profiles of HT29 cells treated with Instant Caffeinated Coffee or Caffeic Acid versus control.	0.62	0.54	0.52	0.73	0.65	0.68	0.46	0.65	0.55
146	GSE48616	Expression data from hBMSCs cultured on PLLA nanofibers	0.73	0.74	0.51	0.73	0.65	-0.10	0.72	0.78	0.77
147	GSE8597	Gene expression analysis of hormone treated MCF7 breast cancer cells in the presence or absence of cycloheximide	0.72	0.70	-0.29	0.73	0.72	0.72	0.66	0.76	0.76
148	GSE47920	Expression data from T lymphocytes derived from T-iPS and peripheral blood	0.70	0.66	0.25	0.70	0.74	0.33	0.58	0.73	0.67
149	GSE9212	Overexpression of lung developmental transcription factors TTF-1, NKX2-8 and PAX9	0.70	0.69	0.18	0.53	0.61	0.63	0.58	0.69	0.48
150	GSE19123	Lactic acidosis triggers starvation response with distinct metabolic profiles	0.66	0.63	0.53	0.63	0.62	0.36	0.48	0.67	0.68
151	GSE25148	Changes in gene expression in HEK-TLR2 cells in response to Helicobacter pylori lipopolysaccharide	0.68	0.66	0.59	0.59	0.55	0.52	0.44	0.70	0.61
152	GSE13330	Senescent Stromal-Derived Osteopontin Promotes Preneoplastic Cell Growth	0.59	0.61	0.70	0.57	0.04	0.70	0.68	0.75	0.75
153	GSE57634	Molecular effects of EtOH and Nicotine on normal human oral keratinocytes	0.61	0.28	0.68	0.60	0.58	0.53	0.60	0.66	0.23

154	GSE26704	p38alfa and ATF2 act differentially depending on DUSP1 expression in NCSCL in response to cisplatin	0.70	0.66	0.52	0.51	0.54	0.61	0.45	0.73	0.68
155	GSE37136	Gene expression profiling of enforced HOXA1 expression in melanoma cell line	0.73	0.72	0.73	0.74	0.74	0.74	-0.55	0.77	0.69
156	GSE27316	Effects of long dsRNA expression in HeLa and HEK293 cells	0.73	0.72	0.32	0.71	0.71	0.73	-0.09	0.77	0.69
157	GSE60771	Testing gene expression changes in VCaP upon depletion of the mutated ETS transcription factor ERG	0.66	0.50	0.62	0.67	0.71	0.67	-0.02	0.71	0.67
158	GSE11418	Passage dependent gene expression in normal human dermal fibroblasts	0.66	0.61	0.28	0.54	0.63	0.43	0.68	0.75	0.67
159	GSE31534	Gene expression profile in A375 melanoma cells after 45 functionally important molecules were knocked down using siRNA	0.67	0.67	0.58	0.66	0.67	0.56	-0.04	0.71	0.67
160	GSE7268	Cryptosporidium infection of human intestinal tissues causes increased expression of Osteoprotegerin	0.66	0.61	0.49	0.61	0.45	0.60	0.47	0.59	0.55
161	GSE14334	Transcriptomic analysis of human lung development	0.60	0.65	0.63	0.61	0.65	-0.09	0.65	0.68	0.71
162	GSE13491	Therapeutic efficacy of human umbilical cord blood-derived mesenchymal stem cells in myocardial repair after infarction	0.71	0.63	0.66	0.66	0.69	0.63	-0.29	0.75	0.72
163	GSE42924	Expression data from immature dendritic cells (iDC) expressing HIV-1 Tat alleles and mutants	0.58	0.67	0.49	0.28	0.61	0.50	0.55	0.71	0.61
164	GSE12198	Primary NKcells vs. NKAES-derived NK cells vs. NKcells stimulated by low/high dose IL2 after 7days of culture	0.67	0.29	0.33	0.68	0.67	0.50	0.54	0.74	0.73
165	GSE20538	Gene expression profiles of fibroblasts from MCT8 patients	0.69	0.63	0.36	0.68	0.62	0.43	0.25	0.73	0.71
166	GSE47746	Gene expression data of fibroblasts transduced with LacZ or p63+KLF4.	0.71	0.71	0.53	0.68	0.64	-0.06	0.45	0.76	0.64
167	GSE23586	Altered gene expressions of leukocyte transendothelial migration and cell communication pathways in periodontitis-affected gingival tissues	0.67	0.31	0.69	0.70	0.52	0.72	0.45	0.79	0.64
168	GSE11407	SCFA-hexosamine scaffold	0.50	0.61	0.66	0.44	0.50	0.46	0.48	0.72	0.65
169	GSE4984	Monocyte Derived Dendritic Cell Maturation	0.59	0.56	0.17	0.65	0.64	0.49	0.59	0.52	0.38
170	GSE45426	Transcriptional events in human skeletal muscle at the outset of concentric resistance exercise training	0.66	0.57	0.65	0.36	0.62	0.19	0.59	0.68	0.73
171	GSE20433	Effects of T350 phospho- on gene repression activity of EZH2	0.70	0.59	0.65	0.66	-0.23	0.68	0.58	0.76	0.58
172	GSE39762	Genome Wide Profiling of p53 Response to Differentiation or DNA Damage of Human Embryonic Stem Cells	0.71	0.66	0.59	-0.22	0.53	0.65	0.70	0.73	0.65
173	GSE55609	Human meningioma culture	0.69	0.55	0.63	0.56	0.39	0.56	0.24	0.70	0.70
174	GSE7888	Expression data from human mesenchymal stem cells (six batches)	0.63	0.60	0.42	0.50	0.49	0.52	0.46	0.67	0.64
175	GSE34112	Effect of NO-sulindac treatment on hypoxic prostate cancer cells	0.71	0.62	0.40	-0.04	0.57	0.70	0.61	0.71	0.63
176	GSE11869	The genomic response of a human uterine endometrial adenocarcinoma cell line to 17alpha-ethynyl estradiol.	0.51	0.60	0.59	0.42	0.34	0.60	0.46	0.45	0.12
177	GSE7224	Gene expression in tonsil and oral epithelia	0.65	0.36	0.69	0.64	-0.05	0.68	0.56	0.67	0.71
178	GSE53059	Human Subperitoneal Fibroblasts and Cancer Cell Interaction Creates Microenvironment Enhancing Tumor Progression and Metastasis	0.66	0.65	0.68	0.65	0.44	-0.20	0.62	0.72	0.70
179	GSE27041	OXPHOS complex I deficiency leads to transcriptional changes of the Nrf2-Keap1 pathway and selenoproteins.	0.58	0.59	0.29	0.63	0.55	0.34	0.49	0.64	0.51
180	GSE4587	Whole-genome expression profiling of melanoma progression.	0.69	0.67	0.39	0.66	0.65	0.51	-0.09	0.72	0.69
181	GSE11622	Molecular Analysis of the Vaginal Response to Estrogens in the Ovariectomized Rat and Postmenopausal Woman	0.68	0.61	0.45	0.34	0.22	0.66	0.51	0.73	0.66
182	GSE42253	Gene expression data from T cells and NK cells with and without treatment with Hsp90 inhibitor (Geldanamycin)	0.71	0.70	0.61	-0.02	0.63	0.68	0.19	0.75	0.72
183	GSE4237	Hussaini-2R01NS035122-06A1	0.60	0.57	0.61	0.63	0.60	0.54	-0.11	0.72	0.43
184	GSE24235	Skeletal muscle gene expression in response to resistance exercise: sex specific regulation	0.56	0.46	0.55	0.41	0.65	0.36	0.42	0.56	0.53
185	GSE30806	Expression profiling in VCP-associated myopathy	0.59	0.52	0.50	0.25	0.48	0.47	0.64	0.55	0.61

186	GSE15543	Meta analysis of gene expression in human islets after in vitro expansion.	0.68	0.50	0.57	0.55	0.52	0.16	0.39	0.70	0.64
187	GSE33643	Comparison of gene expression alterations induced by distinct PI3K inhibitors	0.46	0.54	0.66	0.62	0.33	0.33	0.41	0.64	0.61
188	GSE46914	IDENTIFICATION OF BIOMARKERS OF RESPONSE TO IFNG DURING ENDOTOXIN TOLERANCE: APPLICATION TO SEPTIC SHOCK	0.53	0.57	0.64	0.48	0.42	0.09	0.62	0.52	0.54
189	GSE36895	Molecular Genetic Classification of clear-cell Renal Cell Carcinoma (ccRCC) based on the Gene Expression Profiling of Tumors and Tumorgrafts deficient for BAP1 or PBRM1	0.65	0.55	0.41	0.46	0.50	0.47	0.41	0.58	0.59
190	GSE44596	The effect of Sparstolonin B (SsnB) on gene expression in HCAECs	0.67	0.65	0.63	0.65	0.65	0.68	-0.61	0.71	0.68
191	GSE57463	SOX9 overexpression in melanoma	0.66	0.68	-0.54	0.68	0.59	0.62	0.61	0.72	0.67
192	GSE19315	Global transcriptional response of macrophage-like THP-1 cells	0.65	0.66	-0.36	0.69	0.57	0.63	0.51	0.69	0.73
193	GSE16354	Infection of Lymphatic and Blood Vessel Endothelial Cells (LEC and BEC) with KSHV	0.64	0.47	0.33	0.56	0.57	0.36	0.38	0.64	0.69
194	GSE13487	Antitumor efficacy of RAF inhibitor GDC-0879 involving BRAFV600E mutational status and ERK/MAPK pathway suppression	0.61	0.42	0.59	0.45	0.58	0.55	0.09	0.58	0.18
195	GSE23994	A molecular signature of normal breast epithelial and stromal cells from Li-Fraumeni syndrome mutation carriers	0.66	0.65	0.62	0.57	0.65	-0.50	0.63	0.73	0.70
196	GSE36807	Genome-wide analysis of Crohn's disease and ulcerative colitis biopsy samples.	0.36	0.52	0.43	0.56	0.49	0.64	0.42	0.23	0.59
197	GSE23849	The ERAD inhibitor Eeyarestatin I is a bifunctional compound with an ER localizing domain and a p97/VCP inhibitory group	0.68	0.68	0.39	-0.08	0.50	0.49	0.65	0.72	0.63
198	GSE33301	Expression data from control and COUP-TFII siRNA treated HUVEC cells	0.74	0.51	0.73	0.52	0.62	0.69	0.12	0.77	0.69
199	GSE14897	Highly Efficient generation of Human Hepatic Cells from Induced Pluripotent Stem Cells.	0.63	-0.08	0.63	0.59	0.58	0.62	0.27	0.70	0.66
200	GSE43489	Expression profile from PCE-Epi and derived cell lines	0.82	0.67	0.79	0.81	0.80	0.60	0.49	0.75	0.79
201	GSE46268	Gene expression profile of human monocytes stimulated with all-trans retinoic acid (ATRA) or 1,25a-dihydroxyvitamin D3 (1,25D3)	0.61	0.51	-0.21	0.60	0.59	0.63	0.47	0.66	0.57
202	GSE13376	Exposure of Barrett's associated adenocarcinoma cell lines SKGT4 to deoxycholic acid (DCA)	0.64	0.57	-0.49	0.65	0.63	0.62	0.58	0.61	-0.15
203	GSE27850	HAV acute infection in chimpanzees	0.60	0.35	0.52	0.27	0.51	0.43	0.52	0.60	0.60
204	GSE59412	A Systems Biology Approach identified different regulatory networks targeted by KSHV miR-K12-11 in B cells and endothelial cells	0.64	0.56	0.57	0.66	0.64	-0.45	0.57	0.67	0.64
205	GSE3397	RSV gene expression	0.65	0.63	0.39	0.14	0.16	0.65	0.57	0.70	0.22
206	GSE52674	expression data of miR-21 knockdown in MCF-7	0.51	0.66	0.65	0.65	0.58	0.63	-0.51	0.59	0.64
207	GSE49967	Variability in functional p53 reactivation by Prima-1Met/APR-246 in Ewing sarcoma	0.64	0.58	0.67	0.44	0.72	0.48	0.49	0.58	0.69
208	GSE55859	Gene expression profile of TRAIL-sensitive and -resistant H460 cells	0.67	0.66	0.66	0.67	0.67	0.63	-0.84	0.71	-0.18
209	GSE13637	Influenza virus infected HUVEC	0.39	0.59	0.40	0.15	0.58	0.55	0.46	0.60	0.37
210	GSE31980	Transcriptome profile in the human synovial MSC-aggregates	0.66	0.64	0.60	0.63	0.66	-0.71	0.62	0.70	0.71
211	GSE45512	Human Alopecia Areata Skin Profiling	0.61	0.57	0.65	0.62	-0.45	0.55	0.56	0.66	0.70
212	GSE20141	Expression analysis of laser-dissected SNpc neurons in Parkinson's disease	0.61	-0.22	0.58	0.60	0.54	0.61	0.38	0.67	0.61
213	GSE17032	Expression data from human fibroblasts	0.56	0.58	0.37	0.53	0.51	0.22	0.31	0.64	0.47
214	GSE41364	Expression data for HT29 cells treated with 5-aza-deoxy-cytidine [Affymetrix]	0.57	0.53	0.63	0.53	-0.09	0.66	0.49	0.46	0.28
215	GSE16870	HeLa cells treated with V-ATPase inhibitors or with desoxyferramine compared to HeLa in DMSO or medium with low LDL	0.51	0.64	0.59	0.44	0.58	0.61	-0.32	0.62	0.58
216	GSE48311	Time-dependent changes in gene expression after endotoxinic challenge followed by LR12-scrambled or LR12 treatment.	0.59	0.49	0.17	0.48	0.38	0.37	0.55	0.62	0.35

217	GSE11142	Nicotine effect on CEM model T cell line (kuo-affy-human-232861)	0.61	0.38	-0.07	0.59	0.56	0.32	0.63	0.60	0.62
218	GSE49953	Expression data from two breast cancer cell lines	0.66	0.63	0.66	0.63	0.66	0.65	-0.89	0.70	0.68
219	GSE33630	Normal thyrocytes vs papillary vs anaplastic thyroid carcinomas	0.63	0.58	0.59	0.55	0.58	0.26	0.61	0.44	0.75
220	GSE14987	Expression data from ERBB2 over-expression and EGF stimulation in MCF10A cells	0.64	0.66	0.64	0.63	0.60	0.61	-0.83	0.68	0.67
221	GSE5081	Expression data from Helicobacter positive and negative human gastritis samples	0.56	0.28	0.49	0.52	0.34	0.48	0.28	0.64	0.55
222	GSE36765	Gene expression profiling of CD4+ T cells infiltrating human breast cancer (Discovery Set)	0.59	0.54	0.53	0.39	0.11	0.38	0.41	0.62	0.64
223	GSE49628	Large-scale hypomethylated blocks associated with Epstein-Barr virus-induced B-cell immortalization [Expression Array]	0.66	0.50	0.55	0.61	0.47	0.61	-0.38	0.70	0.65
224	GSE12079	Molecular profiling of CD3- CD4+ T-cells from patients with the lymphocytic variant of hypereosinophilic syndrome	0.55	-0.16	0.53	0.43	0.60	0.49	0.47	0.65	0.63
225	GSE12355	Detection of Notch1-IC, Notch2-IC and EBNA2 target genes in human B cells	0.51	0.55	0.26	0.61	0.57	0.24	0.15	0.60	0.58
226	GSE50208	Molecular-guided therapy predictions reveal drug resistance phenotypes and treatment alternatives in malignant peripheral nerve sheath tumors	0.63	0.64	0.60	0.62	0.61	-0.38	0.17	0.69	0.60
227	GSE4406	Gene expression profiling of CD4+ T-cells and GM6990 lymphoblastoid cell lines	0.63	0.62	0.64	0.63	0.62	0.52	-0.79	0.68	0.68
228	GSE33325	Gene expression changes in human cardiomyocytes exposed to VX (O-ethyl S-[2-(diisopropylamino)ethyl] methylphosphonothiolate)	0.60	0.55	0.60	0.51	0.32	0.59	-0.32	0.64	0.62
229	GSE17549	Loss-of-function mutations in REP-1 affect intracellular vesicle transport in fibroblasts and monocytes of CHM patients	0.53	0.58	0.60	0.61	0.43	-0.31	0.42	0.57	0.57
230	GSE19963	Expression data from hyperplastic polyps and normal colonic mucosa from patients with familial and sporadic HPPS	0.59	0.51	0.44	0.60	0.38	0.61	-0.29	0.64	0.46
231	GSE18934	Gene expression in fetal mesenchymal stem cells for identification of epitopes suitable for non-invasive isolation	0.63	0.62	0.61	0.63	0.62	-0.92	0.64	0.68	0.64
232	GSE21483	Regulation of HB-EGF by miR-212 and acquired cetuximab-resistance in head and neck cancer	0.58	0.61	0.62	0.63	0.62	0.64	-0.91	0.44	0.64
233	GSE16464	Chondrogenic differentiation potential of OA chondrocytes and their use in autologous chondrocyte transplantation	0.52	0.54	0.27	0.57	0.51	-0.03	0.50	0.63	0.56
234	GSE36767	Gene changes of CD4+ T cells infiltrating human breast cancer in the absence of tumor environment (Confirmation Set 24h)	0.64	0.63	0.57	0.58	0.42	-0.65	0.60	0.67	0.69
235	GSE18931	The biological and molecular heterogeneity of breast cancers correlate with their cancer stem cell content	0.60	0.58	0.58	0.45	-0.53	0.43	0.62	0.67	0.64
236	GSE37603	Identification of WISP1 as an important survival factor in human mesenchymal stem cells	0.62	0.58	0.57	-0.46	0.60	0.47	0.49	0.48	0.62
237	GSE15192	Differences between CD44+/CD24- and CD44-/CD24+ subpopulation of immortalized human mammary epithelial cells	0.59	0.62	0.62	0.61	0.57	-0.93	0.61	0.61	0.01
238	GSE40241	Expression data from Versican (VCAN) protein treated ovarian cancer cell line OVCA433	0.59	0.55	0.55	0.61	0.58	-0.73	0.61	0.69	0.58
239	GSE18912	Expression profiling of breast cancer cell lines MCF-7 and MCF-7R4	0.56	-0.49	0.61	0.46	0.50	0.56	0.49	0.63	0.65
240	GSE10289	Cells silenced for SDHB expression and tumor phenotype	0.60	0.62	-0.87	0.55	0.59	0.62	0.59	0.30	0.45
241	GSE15205	TGF or TNF Time series in ARPE19	0.56	0.56	0.48	0.58	0.55	-0.44	0.36	0.66	0.64
242	GSE20948	The Effect of Hepatitis C Virus Infection on Host Gene Expression	0.57	0.58	0.46	-0.13	0.56	0.44	0.15	0.61	0.57
243	GSE11428	Expression data from LNCaP and abl cells	0.52	0.33	0.27	0.37	0.48	0.44	0.22	0.61	0.48
244	GSE35659	A transcriptional map of the impact of endurance exercise training on skeletal muscle phenotype (resting muscle after endurance training)	0.39	0.50	0.50	0.12	0.34	0.20	0.55	0.48	0.58
245	GSE31912	Gene expression profile in MCF7 breast cancer cells after 78 functionallly important molecules were knocked down using siRNA.	0.51	0.54	0.45	0.49	0.37	0.31	-0.05	0.54	0.33

246	GSE11919	Vitamin C-induced gene expression profiling in GM5659 human skin fibroblasts	0.59	0.49	0.66	0.69	0.48	-0.01	0.64	0.70	0.61
247	GSE34628	Gene expression timecourse from Dengue virus infected human endothelial cells	0.67	0.77	0.67	0.63	0.68	0.55	0.43	0.57	0.73
248	GSE11510	Taxonomy of placenta cells	0.55	0.58	0.54	0.48	0.35	0.46	-0.41	0.64	0.32
249	GSE17251	human	0.57	0.53	0.57	0.07	0.35	0.48	-0.03	0.59	0.58
250	GSE21545	Biobank of Karolinska Endarterectomy (BiKE)	0.59	0.57	0.59	0.52	0.53	-0.73	0.52	0.62	0.64
251	GSE9055	Time course gene expression of HUVEC after TNF-alpha treatment	0.50	0.53	0.48	0.15	0.50	0.04	0.31	0.46	0.49
252	GSE35716	4HC]	0.56	0.58	0.56	0.52	0.54	-0.64	0.38	0.61	0.63
253	GSE17385	Gene expression profiling from MM1.S cells with control or beta-catenin knockdown.	0.61	-0.62	0.09	0.59	0.60	0.60	0.61	0.66	0.66
254	GSE30531	Expression data of A375 melanoma cells after DMSO or MLN4924 treatment from 1 hour to 24 hour	0.56	0.50	0.45	0.19	0.56	0.34	-0.14	0.64	0.30
255	GSE2964	Motexafin Gadolinium and Zinc Induce Oxidative Stress Responses and Apoptosis in B-Cell Lymphoma Lines	0.49	-0.33	0.51	0.54	0.39	0.54	0.31	0.61	-0.05
256	GSE8192	The DExH-box RNA helicase RHAU is a Nuclear Protein Involved in Transcription and mRNA Decay	0.38	0.52	0.52	0.37	0.44	0.57	-0.39	0.61	0.48
257	GSE4316	Genome-wide expression profile of human trabecular meshwork cultured cells, non-glaucomatous and POAG tissue	0.64	0.58	0.72	0.74	0.65	0.11	0.69	0.79	0.79
258	GSE6281	Gene expression time-course in the human skin during elicitation of allergic contact dermatitis	0.54	0.53	0.54	0.47	0.37	0.36	-0.25	0.60	0.57
259	GSE18995	Expression data from donor lungs of cardiac death and brain death donors	0.37	0.38	0.44	0.20	0.25	0.28	0.47	0.41	0.25
260	GSE11430	AffymetrixDataset	0.50	0.59	0.53	0.58	0.56	-0.59	0.18	0.58	0.61
261	GSE9927	Chronic CD4+ T cell Activation & Depletion in HIV-1 Infection: Type I Interferon-Mediated Disruption of T Cell Dynamics	0.45	0.37	-0.11	0.43	0.52	0.43	0.25	0.54	0.47
262	GSE10315	Multipotent mesenchymal stromal cells: identification of pathways common to TGFŒ≤3/BMP2-induced chondrogenesis	0.46	0.51	0.45	0.34	0.45	-0.29	0.41	0.54	0.61
263	GSE14491	TGFŒ≤/mutant-p53 jointly controlled genes	0.55	0.39	0.55	0.53	0.45	-0.03	-0.16	0.59	0.61
264	GSE6519	Microarray Analysis of Baboon neonates consuming long-chain polyunsaturated fatty acid formula	0.59	-0.09	0.05	0.55	0.46	0.61	0.50	0.66	0.21
265	GSE4107	Expression profiling in early onset colorectal cancer	0.19	0.48	0.42	0.39	0.41	-0.13	0.48	0.06	0.44
266	GSE11292	High-time-resolution dynamic analysis of human regulatory T cell (Treg) / CD4+ T-effector cell (Teff) activation	0.48	-0.01	0.13	0.49	0.44	0.37	0.30	0.52	0.47
267	GSE11959	Anti-IGF-IR antibody h10H5 induces a unique transcriptional profile in SK-N-AS human neuroblastoma xenograft tumor	0.65	0.41	0.60	0.47	0.58	-0.01	0.38	0.71	0.63
268	GSE27838	Gene expression of expanded and non-expanded natural killer cells from healthy donor and myeloma patients	0.51	0.44	-0.55	0.50	0.52	0.48	0.16	0.60	0.59
269	GSE41828	TWEAK-treated time course in U2OS cells.	0.49	0.48	0.42	0.46	0.34	0.45	-0.64	0.53	0.43
270	GSE41663	Re-analysis by microarray using cDNA target of samples from psoriasis patients enrolled in an etanercept trial	0.54	0.30	0.50	0.45	-0.08	0.51	-0.23	0.57	0.55
271	GSE44029	Expression data from SW480 cells with Gankyrin knockdown	0.52	0.04	0.53	0.49	-0.66	0.52	0.54	0.54	0.55
272	GSE23103	HeLa SCY1-like 1 esiRNA knockdown	0.60	0.60	0.59	0.59	0.57	0.55	-0.90	0.67	0.64
273	GSE39059	Changes in microRNA and mRNA expression with differentiation of human bronchial epithelial cells [mRNA]	0.14	0.50	0.55	0.50	0.52	0.53	-0.77	-0.26	0.59
274	GSE28005	Charaterization of the initial molecular events of adipose tissue development and growth during overfeeding in humans	0.54	0.53	0.53	0.42	0.23	0.10	0.25	0.60	0.55
275	GSE48350	Alzheimer's Disease Dataset	0.47	-0.18	0.45	0.35	0.34	0.41	0.07	0.51	0.41
276	GSE30188	Rho transcription inhibitor CCG-1423 effect on PC-3 cells	0.51	0.49	-0.66	0.51	0.48	0.51	0.06	0.59	0.55
277	GSE37364	Expression data from human colonic biopsy samples (adenoma-carcinoma)	0.23	0.24	0.10	0.46	0.25	0.43	0.24	0.37	0.19

278	GSE18271	Analysis of TALE homeobox genes in neuroblastic tumors: ganglioneuroblastoma and ganglioneuroma	0.48	-0.53	0.50	0.41	0.39	0.41	0.19	0.56	0.38
279	GSE47855	Gene expression analysis for CD56- T, NK, CD56+ T cells, and iNKT cells	0.35	0.35	-0.01	0.32	0.34	0.39	0.10	0.54	0.56
280	GSE10718	Time course of NHBE cells exposed to whole cigarette smoke (full flavor)	0.43	0.48	-0.15	0.21	0.39	0.42	0.01	0.48	0.27
281	GSE7637	Expression data from human mesenchymal stem cells (#4F1560)	0.43	0.46	0.49	0.28	0.47	-0.50	0.18	0.57	0.47
282	GSE20297	The effects of terbutaline or GW9508 on TNF-alpha and IFN gamma (TNF-alpha + IFN gamma) stimulation by HaCaT	0.49	0.47	0.45	0.47	0.11	0.48	-0.71	0.57	0.56
283	GSE10879	Expression data of hormone-responsive MCF-7 cells versus estrogen-deprived MCF-7:5C and MCF-7:2A breast cancer cells	0.34	0.52	-0.04	0.49	0.40	-0.45	0.50	0.40	0.50
284	GSE47685	Gene silencing of BSK65-MONO1 (RNF185) and of its natural antisense RNA (RNF185-AS) using siRNAs	0.66	0.57	0.67	0.67	-0.21	0.58	0.46	0.65	0.43
285	GSE8671	Transcriptome profile of human colorectal adenomas.	0.44	0.12	0.22	0.44	0.37	0.47	0.04	0.46	0.33
286	GSE13070	Human Insulin Resistance and Thiazolidinedione-Mediated Insulin Sensitization	0.46	0.44	0.45	0.00	0.44	-0.46	0.41	0.54	0.53
287	GSE33950	SHARP1 suppresses breast cancer metastasis by promoting degradation of hypoxia-inducible factors	0.40	0.50	0.49	0.37	0.25	-0.80	0.49	0.34	0.22
288	GSE17612	Comparison of post-mortem tissue from brain BA10 region between schizophrenic and control patients.	0.37	-0.30	0.41	0.31	0.20	0.36	0.28	0.44	0.36
289	GSE49910	An Expression Atlas of Human Primary Cells: Inference of Gene Function from Coexpression Networks	0.50	0.44	0.43	0.46	0.44	-0.16	-0.44	0.57	0.53
290	GSE41296	Characterization of Formaldehyde's Genotoxic Mode of Action by Gene Expression Analysis in TK6 Cells	0.45	-0.19	0.19	0.45	0.43	0.38	-0.11	0.53	0.51
291	GSE42046	TWEAK-treated time course in ACHN cells	0.49	0.45	0.32	0.40	0.42	0.27	-0.78	0.57	0.45
292	GSE10311	Systematic Assessment of Human Osteoblast Transcriptome in Resting and Induced Primary Cells	0.62	0.61	0.60	0.08	0.64	0.08	0.61	0.69	0.61
293	GSE15918	Torcetrapib induces aldosterone and cortisol production in an intracellular calcium-dependent mechanism	0.45	0.42	0.47	-0.11	-0.47	0.46	0.32	0.53	0.14
294	GSE11238	Vaccinia E3L mutant virus infected HeLa cell lines (langl-affy-human-215499)	0.42	0.35	0.06	0.46	0.45	-0.46	0.23	0.53	0.15
295	GSE12548	EMT Time series in ARPE19	0.38	0.47	0.39	0.39	0.45	-0.60	0.15	0.56	0.43
296	GSE20318	YWHAZ is an Invasion and Metastasis promoting genes of Lung cancer	0.76	0.72	0.51	0.72	0.68	-0.09	0.74	0.78	0.45
297	GSE15013	Expression of HOXB genes is significantly different in acute myeloid leukemia with a partial tandem duplication of MLL vs. a MLL translocation: a cross-laboratory study	0.39	-0.11	0.39	0.40	0.31	0.19	-0.18	0.47	0.51
298	GSE3202	MK886 treatment of H720 non-small cell lung cancer cell line	0.42	-0.04	0.24	0.42	0.46	-0.21	0.29	0.49	0.23
299	GSE32473	Gene expression is differently affected by pimecrolimus and betamethasone in lesional skin of atopic dermatitis.	0.36	0.37	0.40	0.35	-0.15	0.37	-0.34	0.50	0.36
300	GSE47751	Early tissue responses to etanercept in psoriasis lesions	0.43	0.22	0.38	0.36	-0.04	0.38	-0.38	0.47	0.39
301	GSE33050	GlcNAcylation of histone H2B facilitates its monoubiquitination [Affymetrix data]	0.43	0.39	0.39	0.49	0.24	0.45	-0.80	0.51	-0.05
302	GSE13564	Gene expression in the human prefrontal cortex during postnatal development	0.43	-0.25	0.42	0.31	0.36	-0.34	0.37	0.51	0.45
303	GSE5563	Gene expression profile of VIN lesions in comparison to controls	0.46	0.22	0.36	0.33	0.36	0.39	-0.54	0.50	0.49
304	GSE32876	Inferring transcriptional and microRNA-mediated regulatory programs in glioblastoma	0.35	0.39	-0.16	0.09	0.41	0.33	-0.25	0.42	0.40
305	GSE8056	Gene Expression Profiles in Thermally Injured Human Skin: A Temporal Microarray Analysis	0.45	0.41	0.49	0.47	0.52	0.37	-0.52	0.59	0.41
306	GSE27390	Human bone marrow-derived mononuclear cells (BMMC): rheumatoid arthritis vs. osteoarthritis	0.37	0.38	0.39	0.35	0.30	-0.58	-0.14	0.46	0.33
307	GSE15132	Riboflavin depletion impairs cell proliferation in intestinal cells: Identification of mechanisms and consequences	0.38	0.45	0.22	0.37	0.35	-0.20	-0.27	0.50	-0.02
308	GSE44765	Global profiling of human hair follicle scalp dermal papilla cells using Affymetrix microarrays	0.75	0.69	0.69	0.42	0.76	0.70	0.41	0.80	0.82

309	GSE51524	LNCaP prostate cancer cell lines overexpressing wild-type or GARRPR-mutant Bag-1L	0.38	-0.56	0.37	0.40	0.39	-0.36	0.35	0.47	0.47
310	GSE32526	Expression data from breast cancer tumor-initiating cells	0.40	0.40	0.28	0.40	0.40	-0.28	-0.66	0.43	0.17
311	GSE8687	Inhibition of activation of Sez-4 cell line with IL-2 by Jak kinase inhibitors.	0.32	0.29	0.28	0.36	-0.17	0.30	-0.47	0.33	0.13
312	GSE7216	Cytokine treated normal human epidermal keratinocytes	0.28	0.07	0.28	0.18	0.01	0.37	-0.32	0.43	0.31
313	GSE3151	Oncogene Signature Dataset	0.16	0.22	0.25	0.06	-0.02	0.07	0.12	0.29	0.28
314	GSE12293	Evolution of neuronal and endothelial transcriptomes in primates	0.37	-0.42	0.36	0.30	-0.38	0.33	0.29	0.44	0.41
315	GSE49353	Evaluating cross-hybridization of murine cDNA to the Affymetrix Human Genome U133 Plus 2.0 chipset	-0.33	0.25	0.25	0.34	0.32	-0.45	0.33	-0.09	-0.19
316	GSE15520	The Role of Cholesterol Pathways in Norovirus Replication	0.28	0.53	0.42	0.50	0.54	0.44	-0.77	0.28	-0.13
317	GSE22779	Gene expression data of non-leukemic individuals before and during in-vivo glucocorticoid treatment	0.25	-0.02	0.01	0.23	0.24	-0.16	0.02	0.36	0.38
318	GSE31681	Human cumulus cells	0.30	0.28	0.23	0.06	0.00	-0.38	0.23	0.40	0.27
319	GSE34599	In-transit extremity melanoma III	0.54	0.50	0.52	0.26	0.18	0.21	0.35	0.60	0.53
320	GSE13987	Profile of rolipram treated B-CLL, normal B, and normal T cells	0.28	0.25	0.30	-0.37	-0.54	0.28	0.26	0.39	0.37
321	GSE24337	The Human Airway Epithelial Basal Cell Transcriptome	-0.14	0.19	-0.07	0.21	0.26	0.22	-0.24	0.03	0.25
322	GSE10739	LPS and PMA response in parental MM6 cells	0.34	0.33	-0.64	0.33	0.33	0.33	-0.55	0.44	-0.25
323	GSE11864	Effect of interferon-gamma on macrophage differentiation and response to Toll-like receptor ligands	0.32	0.31	0.20	0.20	0.28	-0.47	-0.53	0.42	0.37
324	GSE29368	CD140a+ human oligodendrocyte progenitor cells	0.29	-0.40	0.23	-0.48	0.25	0.08	0.25	0.33	0.36
325	GSE46873	Dual targeting of MYC and CYCLON by BET bromodomain inhibition optimizes Rituximab response in lymphoma.	0.45	0.38	-0.58	0.26	0.41	0.43	0.31	0.37	0.21
326	GSE15824	Gene expression profiling of human gliomas and human glioblastoma cell lines	0.26	0.24	-0.03	0.28	0.30	0.19	-0.44	0.39	0.23
327	GSE8139	Expression data from MCF7/HER2-18 xenografts	0.03	0.10	-0.03	-0.04	0.06	-0.04	0.13	0.13	0.21
328	GSE33585	Expression data from monocytic cell lines (THP)	0.25	0.27	-0.39	0.25	0.05	0.26	-0.58	0.38	0.35
329	GSE19278	2]	0.41	0.29	-0.06	0.36	0.34	0.31	-0.51	0.48	0.48
330	GSE9517	Cysteine deprivation in liver cell line	0.33	0.08	0.32	0.03	0.02	0.37	-0.10	0.31	0.33
331	GSE52158	Dynamic developmental signaling logic underlying lineage bifurcations during human endoderm induction and patterning from pluripotent stem cells [Expression data set]	0.21	0.14	0.22	0.08	-0.38	0.15	-0.33	0.31	0.15
332	GSE24468	Elucidation of the Mechanisms by which the Progesterone Receptor Inhibits Inflammatory Responses in Cellular Models of Breast Cancer	0.12	-0.20	-0.09	-0.03	-0.02	-0.04	0.01	0.27	0.23
333	GSE10070	Gene Expression in MCF10A cells through Differentiation on Transwells	0.32	0.29	-0.41	0.23	0.26	0.31	-0.36	0.36	0.36
334	GSE18235	Effect of 10 Cigarette Smoke Condensates on Primary Human Airway Epithelial Cells	0.44	0.40	-0.32	0.35	0.38	0.45	0.02	0.47	0.30
335	GSE23610	Gene expression profiles of MCF-7 cells treated with Si-Wu-Tang, estradiol and ferulic acid	0.08	-0.32	-0.32	-0.02	0.04	-0.18	0.06	0.17	0.17
336	GSE36701	Gene expression analysis of rectal mucosa in chronic irritable bowel syndrome (IBS) compared to healthy volunteers (HV)	0.39	0.52	0.54	0.57	0.18	0.60	0.53	0.65	0.62
337	GSE17400	Dynamic Innate Immune Responses of Human Bronchial Epithelial Cells against SARS-CoV and DOHV infection	0.35	0.64	0.29	0.50	0.59	0.66	0.59	0.15	0.39
338	GSE40266	Expression data from TGF-beta-treated human ovarian fibroblasts	0.04	-0.33	-0.19	0.03	0.08	-0.37	0.09	0.15	0.02
339	GSE11941	Topoisomerase II inhibition involves characteristic chromosomal expression patterns: Trovafloxacin study	0.65	0.73	0.57	0.52	0.74	0.70	0.47	0.79	0.81
340	GSE53603	Expression data from SKOV3 cells treated with SAHA or vehicle control	0.61	0.51	0.63	0.58	0.43	0.29	-0.09	0.59	0.49
341	GSE10281	Letrozole (Femara) early response to treatment	0.50	0.48	0.44	0.07	0.37	0.50	0.42	0.42	0.52

342	GSE8784	Plasmodium Circumsporozoite Protein Promotes the Development of the Liver Stages of the Parasite	0.28	-0.29	0.19	0.30	0.18	0.29	-0.43	0.42	0.36
343	GSE32967	Modeling lethal prostate cancer variant with small cell carcinoma features [expression profile]	0.65	0.32	0.28	0.61	0.47	0.54	0.63	0.71	0.72
344	GSE25619	Gene expression profiles of granulin- and control-treated normal human mammary fibroblasts	0.72	0.66	0.66	0.26	0.59	0.53	0.41	0.72	0.74
345	GSE16480	Inactivation of CDK2 is synthetic lethal to MYCN-overexpressing cancer cells	0.46	0.56	0.44	0.55	0.53	0.54	-0.05	0.63	0.41
346	GSE9984	Profiling Gene Expression in Human Placentae of Different Gestational Ages: an OPRU Network and UW SCOR Study	0.64	0.64	0.36	0.64	0.65	0.16	0.44	0.63	0.69
347	GSE33495	Disrupted transcripitonal network in ŒîNp63 AEC tissue model [gene expression]	0.67	0.60	0.28	0.61	0.07	0.64	0.24	0.67	0.66
348	GSE12963	Gene expression in human CD4+ T-lymphocytes infected with VSVG-pseudotyped HIV-1 viruses lacking Env, Vpr, and Nef	0.62	0.56	-0.14	0.53	0.45	0.55	0.62	0.63	0.49
349	GSE9250	Genomic profiling in CLL and subtypes of del13q14	0.63	0.21	0.46	0.50	0.51	0.35	0.56	0.63	0.59
350	GSE31215	Gene expression analysis of human pediatric mesenchymal stem cells (hpMSCs) upon expression of EWS-FLI-1	0.45	0.52	0.56	0.49	0.56	0.26	0.44	0.51	0.43
351	GSE4737	HCaRG vs NEO	0.69	0.70	0.66	0.19	0.54	0.51	0.63	0.71	0.63
352	GSE30439	Exposure of cystic fibrosis bronchial epithelial cells (CFBE 41 o-) to Pseudomonas aeruginosa (PA01) biofilms	0.63	0.54	0.27	0.60	0.55	0.57	0.09	0.64	0.60
353	GSE40986	Gene expression profiles induced by overexpression of PDEF in MCF10A mammary epithelial cell line	0.56	-0.39	0.15	0.62	0.58	0.62	0.59	0.52	0.48
354	GSE38718	Sex and aging effect on skeletal muscle transcriptome in humans	0.38	0.39	0.37	-0.08	0.40	-0.16	0.30	0.40	0.40
355	GSE33112	Gene expression in colon cancer stem cells (CSC) cultures identified by Wnt signaling levels	0.62	0.59	0.67	0.62	0.65	0.27	0.36	0.71	0.48
356	GSE8640	TFAP2C regulates multiple pathways of estrogen signaling	0.45	0.56	0.37	0.35	0.35	0.41	-0.17	0.60	0.57
357	GSE22148	Induced Sputum Genes Associated With Spirometroc and Radiological Disease Severity in COPD Ex-smokers	0.43	0.38	0.40	0.43	0.36	-0.22	0.06	0.50	0.50
358	GSE57552	ZFX silencing introduced differential gene expression in leukemia cells	0.47	0.48	0.45	0.30	-0.01	0.48	-0.80	0.53	0.54
359	GSE24530	Identification and Characterization of Subpopulations within Human Embryonic Stem Cell Lines	0.65	0.68	0.70	0.52	0.37	0.30	0.59	0.75	0.61
360	GSE2817	Wavelet modelling of microarray data provides chromosomal pattern of expression which predicts survival in gliomas	0.43	0.27	0.27	0.38	0.16	0.10	0.43	0.57	0.45
361	GSE29330	Identification of GNG7 as An Epigenetically Silenced Gene in Head and Neck Cancer by Gene Expression Profiling	0.59	0.57	0.60	0.26	0.25	0.53	0.23	0.54	0.56
362	GSE33424	Expression data from human cord blood CD161++/CD161+/CD161- CD8+ T cell subsets	0.45	0.13	0.45	0.09	-0.51	0.42	0.40	0.54	0.47
363	GSE41035	FGFR3-shRNA induced transcriptional changes in RT112 bladder cancer cells	0.51	-0.11	0.25	0.49	0.48	0.54	0.15	0.60	0.59
364	GSE31782	Knock-down and Over-expression of JMJD6 in MCF-7 and/or MDA-MB231	0.22	0.52	0.52	0.47	0.47	0.44	-0.38	0.29	-0.08
365	GSE13274	Ad-HER-wt and Ad-HER2-ki infected HMECs	0.51	0.41	0.50	0.12	0.45	0.40	-0.07	0.54	0.57
366	GSE36287	Expression data from primary human keratinocytes exposed to cytokines in vitro (IL-4, IL-13, IL-17A, IFN-alpha, IFN-gamma, TNF)	0.47	0.60	0.52	0.53	0.22	0.60	0.32	0.64	0.21
367	GSE16237	Expression data of human neuroblastoma tissue samples	0.51	0.11	0.47	0.48	0.52	0.19	0.44	0.63	0.47
368	GSE21979	Transcriptional and post-transcriptional regulation of VEGF by the unfolded protein response	0.63	0.60	0.43	0.56	0.56	0.60	-0.23	0.61	0.53
369	GSE39902	Role of TAZ as mediator of Wnt signaling (MII)	0.55	0.52	0.59	0.24	0.54	0.49	-0.13	0.48	0.55
370	GSE8685	Activation of Sez-4 cell line with IL-2, IL-15 or IL-21.	0.20	0.31	0.26	0.28	-0.21	0.34	-0.45	0.43	0.40
371	GSE6140	Cross platform microarray analysis for robust identification of differentially expressed genes	0.01	0.73	0.74	0.73	0.70	0.66	0.70	-0.41	-0.34
372	GSE14668	B-Cell Gene Signature with Massive Intrahepatic Production of Antibodies to	0.55	0.41	0.43	0.60	0.43	0.57	0.39	0.63	0.65

		Hepatitis B Core Antigen in HBV-Associated Acute Liver Failure									
373	GSE11367	Effect of IL-17 on human vascular smooth muscle cells	0.62	0.56	0.54	0.12	0.42	0.58	0.32	0.66	0.72
374	GSE21668	Expression data from undifferentiated human embryonic stem cells (hESC) and Day 3.5 mesodermal progenitor (CD326neg CD56+) population	0.31	0.72	0.61	0.76	0.70	0.55	0.68	0.79	0.75
375	GSE24422	Effect of insulin on the stromal and adipocyte cells within hMSC derived adipocytes	0.60	0.43	0.42	0.18	0.31	0.56	0.04	0.63	0.56
376	GSE41802	Isocitrata Dehydrogenase (IDH) Mutations Promote a Reversible ZEB1/mir-200-Dependent Epithelial Mesenchymal Transition (EMT)	0.42	0.60	0.47	0.50	0.35	0.44	0.45	0.63	0.42
377	GSE5486	Using GINI2 to identify novel mutations in candidate tumor suppressor genes in colon cancer cells	0.60	0.50	0.38	0.07	0.44	0.41	0.49	0.42	0.23
378	GSE19735	Comparison of human embroynic stem cell derived vascular cells to mature human vascular and hematopoietic cells	0.55	0.48	0.37	0.54	-0.05	-0.25	0.55	0.59	0.53
379	GSE7874	Effects of EPO and EST on erythroid maturation	-0.26	0.16	0.11	0.17	0.20	-0.49	0.17	0.15	0.25
380	GSE10046	Breast cancer-associated fibroblasts confer AKT1-mediated epigenetic silencing of Cystatin M in epithelial cells.	0.77	0.82	0.65	0.59	0.57	0.76	0.60	0.83	0.75
381	GSE30127	Establishment of human trophoblast progenitor cell lines from the chorion	0.62	0.06	0.31	0.59	0.64	0.60	0.31	0.56	0.61
382	GSE40873	a prospective study	0.54	0.08	0.55	0.32	0.48	0.48	0.15	0.59	0.60
383	GSE11618	Stable XIAP knockdown in HCT116 colon cancer cells	0.57	0.46	0.27	0.58	0.59	0.50	0.11	0.65	0.66
384	GSE30660	The Effect of Repeated Whole Cigarette Smoke Challenge on Human Air-Liquid Interface Lung Epithelial Cultures	-0.40	0.26	0.22	0.21	0.32	0.33	-0.53	-0.24	-0.04
385	GSE9169	Gene expression during neuronal differentiation in two subtypes of SH-SY5Y	0.51	0.26	0.41	0.52	0.43	0.39	0.25	0.64	0.54
386	GSE44807	Gene expression data from primary human bronchial epithelial cells expressing EGFP or DN-GRHL2	0.61	0.50	0.60	-0.30	0.58	0.04	0.61	0.18	0.65
387	GSE7586	Genome wide analysis of placental malaria	0.38	0.52	0.47	0.06	0.45	-0.20	0.53	0.46	0.56
388	GSE53552	Gene expression profiling in psoriatic lesional and non-lesional skin [brodalumab treatment]	0.50	0.22	0.48	0.34	0.14	0.44	-0.09	0.55	0.51
389	GSE40281	Signaling pathways of HPAIV	0.55	0.61	0.61	0.55	0.31	0.61	0.39	0.64	0.21
390	GSE15773	Expression data from human adipose tissue	0.52	0.42	0.46	0.44	0.11	-0.24	0.39	0.58	0.44
391	GSE39454	Genomic signatures characterize leukocyte infiltration in myositis muscles	0.48	0.42	0.47	-0.01	0.27	-0.28	0.37	0.44	0.55
392	GSE41386	Role of REST in the pathogenesis of uterine fibroids	0.59	0.69	0.40	0.67	0.45	0.63	0.45	0.63	0.63
393	GSE55529	EcadEGFP expression in MDA-MB-134 and IPH-926	0.68	0.54	0.34	0.61	0.46	0.61	0.59	0.58	0.77
394	GSE40730	Genome-wide analysis of RNAs translationally regulated upon BRCA1 depletion in human mammary epithelial cells	0.66	0.67	0.62	0.12	0.31	0.63	0.53	0.66	-0.27
395	GSE27128	Expression levels in strained vs. non-strained Calu-3 lung epithelial cells	0.57	0.61	0.60	0.49	0.53	0.54	-0.14	0.52	0.13
396	GSE32100	Glioma cells oxygen response	0.06	-0.22	-0.07	-0.13	0.05	-0.21	-0.09	0.10	0.10
397	GSE4600	Identifying targets of MeCP2 during neuronal maturational differentiation	0.48	-0.38	0.22	0.41	0.49	0.47	0.53	0.54	0.49
398	GSE10595	Interaction of bone marrow stroma and monocytes: bone marrow stromal cell lines cultured with monocytes	0.69	0.63	0.64	0.67	0.61	-0.47	0.51	0.73	0.01
399	GSE25087	Human Fetal and Adult Peripheral Na√Øve CD4+ T cells and CD4+CD25+ Treg cells	0.57	0.47	0.31	0.44	0.51	-0.45	0.45	0.63	0.61
400	GSE39843	Expression data of cystic fibrosis and non-cystic fibrosis airway cell lines under oxidative stress	0.64	0.58	0.45	0.29	0.46	0.20	0.45	0.66	0.68
401	GSE10575	Migratory chondrogenic progenitor cells from repair tissue during the later stages of human osteoarthritis	0.54	0.52	0.37	0.24	0.50	0.20	-0.19	0.62	0.46
402	GSE5675	Pilocytic astrocytoma	0.42	0.35	0.45	0.38	0.40	0.20	0.45	0.61	0.56
403	GSE23640	Gene-expression profile of breast cancer cell lines and sorted breast cancer epithelial cells	0.50	0.55	0.29	0.30	0.52	0.54	0.20	0.48	0.61
404	GSE4975	Expression data from p63 siRNA in squamous cell lines	0.59	0.58	0.62	0.36	-0.45	0.63	0.38	0.68	0.28

405	GSE40968	The effect of ACSL4 expression on overall gene expression in breast cancer cell lines	0.68	0.61	0.62	0.55	0.31	0.48	0.50	0.70	0.66
406	GSE10580	Genes regulated by PRDM5 in U2OS cells.	0.53	0.50	-0.24	0.57	0.42	0.30	0.57	0.56	0.26
407	GSE34828	Expression data from fibroblast growth factor receptor 4 (FGFR4) knock down ovarian cancer cell lines	0.66	0.70	0.67	0.24	0.35	0.34	0.65	0.61	0.32
408	GSE20086	Heterogeneity of gene expression in stromal fibroblasts of human breast carcinomas and normal breast	0.63	0.30	0.52	0.36	0.39	0.51	0.53	0.67	0.64
409	GSE11729	H1299 EGF and Iressa stimulation	0.49	0.55	0.47	0.53	0.39	0.19	0.05	0.49	0.11
410	GSE50175	Expression data from human Th1 and Th1Th17 cells	0.63	0.06	0.40	0.64	0.55	0.61	0.33	0.66	0.69
411	GSE43177	MicroRNA regulate immunological pathways in T-cells in immune thrombocytopenia (ITP) [mRNA]	0.68	0.16	0.47	0.66	0.32	0.67	0.66	0.71	0.71
412	GSE41485	Expression data of A939572 SCD1 inhibitor treated ccRCC cells	0.54	0.48	0.33	0.42	0.69	0.52	0.54	0.74	0.37
413	GSE35006	Profiling of p53-responsive genes in human breast cancer cells harboring endogenous ts-p53 E285K	0.73	0.53	0.20	0.65	0.66	0.58	0.63	0.70	0.70
414	GSE14474	The Effects of Static Magnetic Fields on Human Embryonic Cells	0.33	0.54	0.60	0.19	0.62	0.28	0.51	0.62	0.54
415	GSE8507	Neutrophil and PBMC gene expression data from Job's Syndrome	0.38	0.38	0.39	0.27	0.33	0.00	-0.15	0.52	0.25
416	GSE9101	Expression data in native lipoprotein-stimulated human THP-1 macrophages	0.29	0.36	0.28	-0.31	-0.43	0.36	0.32	0.44	0.38
417	GSE40215	shRNA knockdown of the transcription factor NF-YA (NFYA)	0.52	0.51	0.54	0.51	0.35	0.54	-0.82	0.59	0.56